Coded Aperture Imaging for Fluorescent X-rays-Biomedical Applications

A. Haboub, A.A.MacDowell, S. Marchesini, D.Y.Parkinson
Lawrence Berkeley National Lab., Berkeley, California 94703, USA

***Abstract*— Employing a coded aperture pattern in front of a charge couple device pixilated detector (CCD) allows for imaging of fluorescent x-rays (6-25KeV) being emitted from samples irradiated with x-rays. Coded apertures encode the angular direction of x-rays and allow for a large Numerical Aperture x-ray imaging system. The algorithm to develop the self-supported coded aperture pattern of the Non Two Holes Touching (NTHT) pattern was developed. The algorithms to reconstruct the x-ray image from the encoded pattern recorded were developed by means of modeling and confirmed by experiments. Samples were irradiated by monochromatic synchrotron x-ray radiation, and fluorescent x-rays from several different test metal samples were imaged through the newly developed coded aperture imaging system. By choice of the exciting energy the different metals were speciated.**

***Index Terms*— Coded aperture, NTHT, Fluorescent x-rays**

I. Introduction

Coded aperture imaging has been used in a variety of x-ray and- γ-ray fields, such as astronomical applications, medical physics [1], plasma imaging [2], and neutron imaging [3]. It is an imaging technique without conventional lenses which was first suggested in 1961 for use in x-ray astronomy cameras [4, 5]. This imaging technique involves the use of high Z-material as the coded aperture pattern or mask, and consists of a known arrangement of transparent and opaque elements. The mask is placed between the x-ray source and a suitable sensitive detector. Transparent elements in the mask act as pinhole cameras to produce an overlapping image on the detector. This imaging technique improves the signal noise ratio (SNR) efficiency of the system over a single pinhole imaging camera.

Coded apertures encode the angular direction of x-rays, and given a known source plane, allow for a large Numerical Aperture x-ray imaging system. The algorithms to develop the self-supported coded aperture pattern of the Non Two Holes Touching (NTHT) and to reconstruct the x-ray image from the encoded pattern recorded have been developed by means of modeling and confirmed by experiments [6].

By choice of exciting x-ray radiation, fluorescent x-rays from several different test metal samples were imaged through the newly developed coded aperture imaging system. We speciate the metals by energy selecting the exciting x-rays which restrict the fluorescent x-rays available for imaging. The current CCD used lacked energy resolution, but we envisage integrating a newly developed energy resolving CCD, which will allow for imaging with elemental specificity of emitted fluorescent x-rays. Further development can include imaging sample sections with x-ray slice illumination of the sample, and by sample scanninga 3D image can be built up.

Uses for such a detector could be speciation of metals in various biological materials. Metals even with small concentration can contaminate the environment, which leads to a considerable growth of interest in trace elemental analyses and monitoring of metals in plants, animal and human tissues. For this reason several techniques has been used for monitoring these trace contaminants, such as: atomic absorption spectroscopy, graphite furnace atomic absorption spectroscopy, and x-ray fluorescence spectroscopy (XRF) [7]. This new detector has the potential to image x-ray fluorescing samples in 3D. By choice of fluorescent x-rays to be > 20 KeV for example, sample thickness can be 10's of mm so could be relevant for 3D imaging of small animals. This study represents the initial work on the detector development that can image and speciate elements in 3D within a sample.

II. THEORETICAL REVIEW AND SIMULATION

Coded aperture imaging is a two-step process. The first step, represented by equation (1), is known as the convolution. It is the generation of an overlapping image or a coded image when photons are being emitted from a source, pass through the transparent elements of the coded aperture pattern and projected onto the detector. The second step, represented by equation (2) and known as the deconvolution, is the decoding or the reconstruction of the image through a suitable reconstruction method that satisfy equation (3)

$$\mathrm{I}(\mathrm{x},\mathrm{y}) = \mathrm{O}(\mathrm{x},\mathrm{y}) \otimes \mathrm{A}(\mathrm{x},\mathrm{y}) \quad (1)$$

$$\mathrm{O}'(\mathrm{x},\mathrm{y}) = \mathrm{O}(\mathrm{x},\mathrm{y}) \otimes \mathrm{A}(\mathrm{x},\mathrm{y}) \otimes \mathrm{D}(\mathrm{x},\mathrm{y}) \quad (2)$$

$$\mathrm{D}(\mathrm{x},\mathrm{y}) \otimes \mathrm{A}(\mathrm{x},\mathrm{y}) = \delta \quad (3)$$

$\mathrm{I}(\mathrm{x},\mathrm{y})$ represents the coded image, $\mathrm{O}(\mathrm{x},\mathrm{y})$ is an object parallel to the coded aperture pattern whose transmission function is $\mathrm{A}(\mathrm{x},\mathrm{y})$, and D(x,y) is a decoding function or anti-mask. For an ideal imaging reconstruction, the convolution of the two

Work was supported by the Director, Office of Science, Office of Basic Energy Sciences, of the U.S. Department of Energy under Contract No. DE-AC02-05CH11231

functions D(x, y) and A(x, y) is a system point spread function (SPSF) that is delta function.

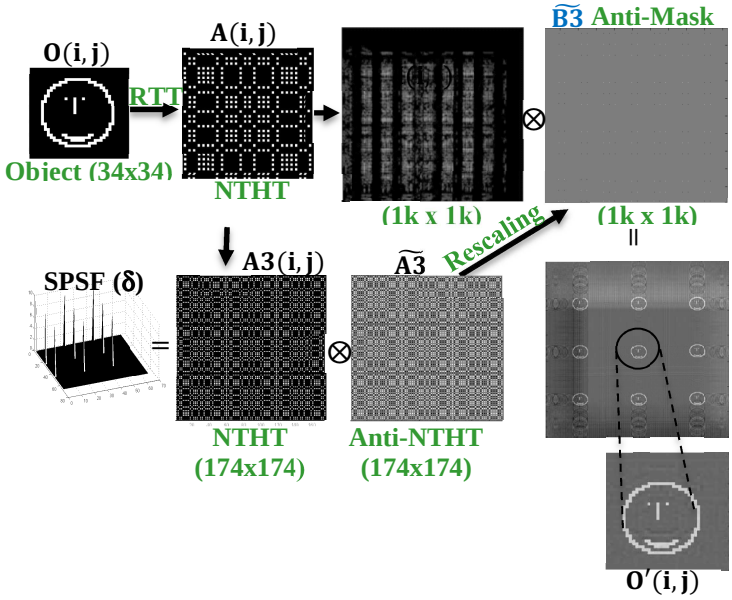

Fig. 1. Coded aperture imaging simulation using ray tracing followed by a newly developed reconstruction techniques that duplicates the mask and derives its anti-mask. Through the same ray tracing procedure, the anti-mask is magnified and rescaled. The image reconstruction is yielded through the Fast Fourier Transform inversion techniques.

This coded aperture imaging technique was modeled by Ray Tracing Technique [6] by simulating the arrangement of the experimental setup that includes a source, the coded aperture pattern and detector. The simulated source is a happy face O(i, j) (Fig.1) while the coded aperture pattern A(i, j) 58x58 is NTHT MURA. The middle of each pixel of the source is ray traced, by passing through the middle of each pinhole of the mask and projected onto the detector. The ray tracing is followed by a newly developed reconstruction technique involving mask duplication A3(i, j), anti-mask $\widetilde{A3}(i, j)$ derivation and magnification, rescaling and Fast Fourier Transform inversion techniques to yield faithful reconstruction of images O′(i, j) by modeling as is shown in Figure 1.

$$\widetilde{A3}(i, j) = \text{iFFT2}(1./\text{FFT2}(A(i, j)); \quad (4)$$

$$O'(i, j) = \text{iFFT2}(\text{FFT2}(I(i, j).* \text{FFT2}(\widetilde{B3}(i, j))) \quad (5)$$

III. EXPERIMENTS AND RESULTS

The experimental setup used to image fluorescent x-rays has been developed [6]. The coded aperture imaging system described in [6], incorporates a square 50-μm thick Tantalum mask of size 5.8 mm that is an arrangement of 421 20-μm holes in 58x58 NTHT MURA and fabricated by laser milling, as it is seen in Figure 2. The detector used is Andor CCD detector of array size 1k x 1k with a pixel size of 13 μm. The detector dimensions are larger than those of the mask, so that this configuration provides a larger fully coded field of view (FCFV). Figure 3 illustrates the conceptual schematic of this experimental setup which is designed for 70 μm resolution over a field of view (FoV) of 6.25 mm x 6.25 mm. The sample-aperture and aperture-detector spacing are $d_1 = 70\ mm$ and $d_2 = 40\ mm$ respectively.

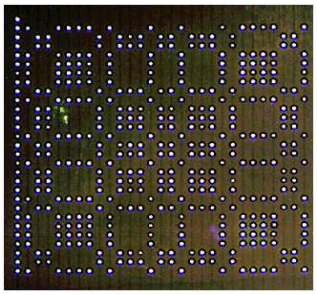

Figure 2. A magnified photograph of the 58 x 58 NTHT used in the coded aperture imaging of fluorescent x-rays. It is a square 50-μm thick tantalum mask of size 5.8 mm that has an arrangement of 421 20-μm holes drilled by a laser miller.

The sample used in this experiment is shown in Figure 4. It consists of eight thin materials (Cr, Fe, Cu, Zn, Ge, Zr, Mo, Ag) ranging from 1-2 mm in sizes and 8 to 15 μm in thickness, and which were glued on a transparent tape. It is placed within the field of view of the system, at an angle of 45° to the x-rays direction, and at the distance d_1 from the coded aperture and $d = d_1 + d_2$ from the detector. The sample is irradiated by monochromatic synchrotron x-rays and the stimulated fluorescent x-rays that pass through the transparent positions of the coded aperture pattern are projected onto the detector, forming a coded image. These materials were chosen based on their fluorescent x-ray energies to test the capabilities of our coded aperture system for screening and imaging different fluorescent x-rays emitted from different materials at different x-ray energies.

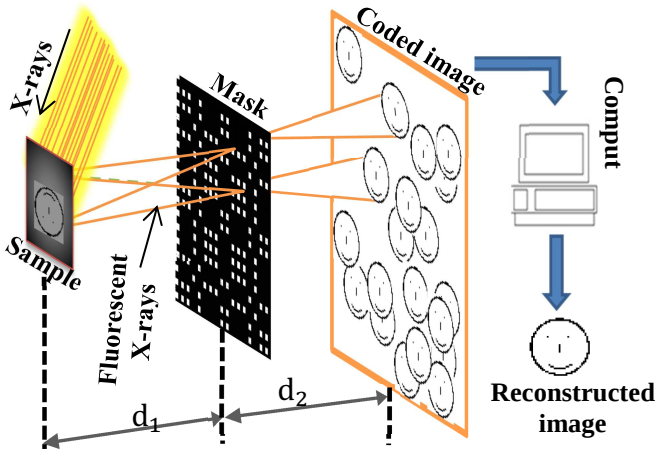

Figure 3. Conceptual schematic of the experimental setup used of coded aperture imaging for fluorescent x-rays emitted from sample when irradiated with x-rays.

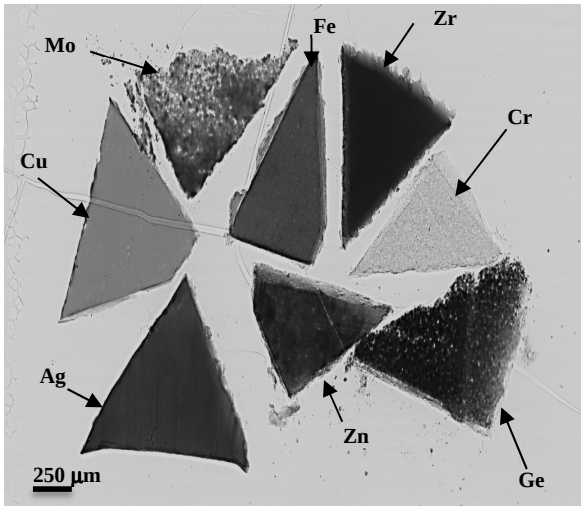

Figure 4. Radiography image of a sample, which consists of several thin metals (Cr, Fe, Cu, Zn, Ge, Zr, Mo, Ag) that emitted fluorescent x-rays (6-25KeV), when irradiated by the synchrotron radiation

At the x-ray micro-tomography Beamline 8.3.2, (Advanced Light Source, Lawrence Berkeley National Lab.) the monochromatic synchrotron x-rays illuminated the eight thin materials, which can emit a wide angular fluorescent x-rays of energies between 6 and 26 keV given adequate exciting x-ray fluorescence x-ray energy. These x-rays pass through the transparent elements of the coded aperture and form a coded image on the detector plan, as it is shown in Figure 5 for the x-ray energies of 6 keV and 26 keV respectively.

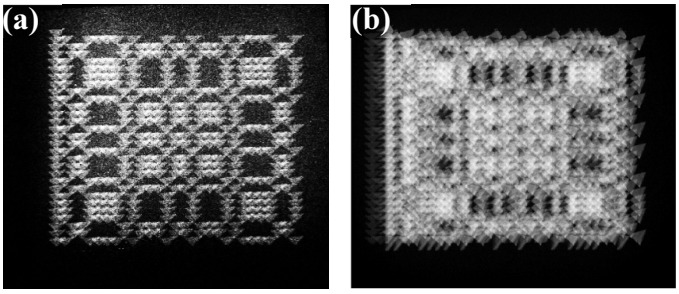

Figure 5. Example of coded images when the test materials are irradiated with x-rays of (a) energy 6 keV, (b) 26 keV.

The images were reconstructed by convoluting the coded images and its corresponding decoding functions which were obtained by the mask duplication, anti-mask derivation, magnification and rescaling process followed by the FFT inversion technique. Figure 6 shows all reconstructed images of fluorescent x-rays of energy between 6 and 25 keV that have being emitted from several materials when irradiated with x-rays radiation of different energies. Table 1 illustrated the fluorescent x-rays emitted from each material depending on the x-rays energies irradiated with. For example at x-ray energy of 6 keV, only excites the Chromium triangle to emit fluorescent x-rays, whereas at 26 keV all materials of the multi-element sample emit the fluorescent x-rays.

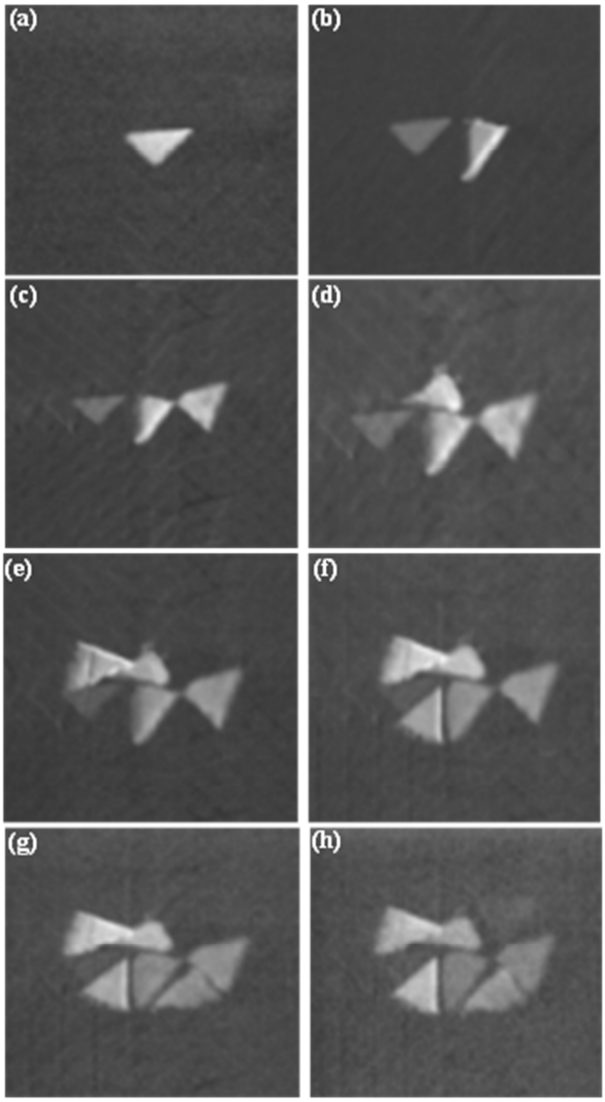

Figure 6. Reconstructed image of fluorescent x-rays (6-25KeV) that have being emitted from several materials when irradiated with x-rays radiation: (a) 6 keV (Cr) (b) 7.2 keV (Cr, Fe) (c) 9.2 keV (Cr, Fe, Cu) (d) 10 keV (Cr, Fe, Cu, and Zn) (e) 12 keV, (Cr, Fe, Cu, Zn, and Ge) (f) 19 keV, (Cr, Fe, Cu, Zn, Ge, and Zr), (g) 21 keV, (Cr, Fe, Cu, Zn, Ge, Zr, and Mo), (h) 26 keV, (Cr, Fe, Cu, Zn, Ge, Zr, Mo, Ag)

X-rays (keV)	Cr	Fe	Cu	Zn	Ge	Zr	Mo	Ag
6	x							
7.2	x	x						
9	x	x	x					
10	x	x	x	x				
12	x	x	x	x	x			
19	x	x	x	x	x	x		
21	x	x	x	x	x	x	x	
26	x	x	x	x	x	x	x	x

Table 1. Representation of fluorescent x-rays emitted from test materials as a function of the synchrotron x-rays energies

The reconstruction images are able to image all the individual metal shapes. Some reconstruction artifacts remain in the images indicating more refinement in the alignment and calibration of geometric distortion. The modulation transfer function (MTF) was measured from the reconstructed images.

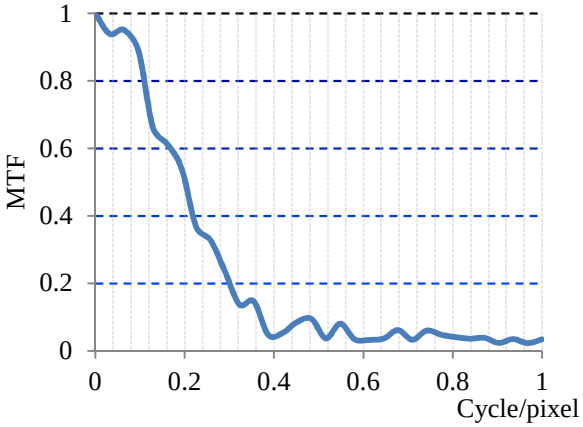

Figure 7. Modulation transfer function (MTF) as a function of cycle/pixel measured from the reconstructed image of Chromium triangle [image (a) of Figure 6.]

Figure 7 shows the MTF of the image (a) of Figure 6 as function of the cycle/pixel. The image sharpness is closely related to the spatial frequency where MTF is 50%. In this image, the 50% of the MTF corresponds to 0.2 cycle/ pixel. The pixel size of the detector is 13 µm, thus the spatial resolution in this decoded image is about ~ 5 pixels (65 µm) at 50% MTF. This resolution is approximately that obtained from simple geometric considerations of d1, d2, the size of the apertures of the mask and CCD pixel size.

IV. Future Developments

The above results indicate the initial promise of the technique. The development of the technique can include the use of an energy resolving CCD [8] to allow for elemental speciation. Improved spatial resolution can be achieved with smaller coded aperture hole size and CCD pixel size. Sensitivity can be improved by changing the current NTHT coded pattern of only 0.4% open area to a MURA pattern of 50% open area. As an example of the sensitivity of the instrument, take for example the case of irradiating a 10 µm sized contaminant of Uranium irradiated with x-rays of energy 20 keV. 80% of this energy is absorbed of which 50% is re-irradiated in the form of Lα fluorescent x-rays. Given a 50% open area, a MURA coded aperture that subtends 1 steradian and accepts 0.5 steradian. The flux density at the synchrotron is around ~10^5 hν/s/µm^2, the 10 µm thick Uranium absorbs ~8.10^6 hν, and re-irradiates ~4.10^5 hν/s into 4π steradian. Flux on the ccd is predicted to be ~15,000 hν/s/. At a Uranium concentration of 0.1% the flux would reduce to 15 hν/s/ requiring several minutes to collect an image. 3D imaging can be developed by scanning an exciting X-ray slice through the sample building up the sample fluorescent images section by section. In this way a 3D element map can be imaged from within samples.

V. Conclusion

The algorithms [6] developed for the self-supported coded aperture pattern of the Non Two Holes Touching (NTHT) were used to reconstruct images of fluorescent x-rays emitted from different test materials when irradiated with x-rays at different energies. The code produced reliable images with a spatial resolution of ~ 65 µm which is approximately that derived from simple geometrical considerations. The instrument can be further developed to include elemental speciation by including an energy resolving CCD [8], improved spatial resolution by the use of smaller coded holes, improved sensitivity by the use of MURA coded apertures and 3D imaging by means of sample illumination with x-ray slices.

VI. Acknowledgement

The Advanced Light Source is supported by the Director, Office of Science, Office of Basic Energy Sciences, of the U.S. Department of Energy under Contract No. DE-AC02-05CH11231.

References

[1] Kazachkov, Yu. P., Semenov, D. S. and. Goryacheva, N. P., "Application of Coded Apertures in Medical gamma-ray Cameras" Instrum. And Exp. Techniques 50 267-274 (2003).

[2] Chen, Y-W, Kishimoto, K.,"Tomography resolution of uniformly redundant arrays coded aperture", Rev. Sci. Instrum. 74, 2232-2235 (2003).

[3] Anderson, I. S., McGreevy, R., Bilheux, H. Z. (Eds.), "Neutron Imaging and Applications", Springer US (2009) ISBN: 978-0-387-78692-6.

[4] Mertz, L., and Young, N. O., [Proc. Int. Conf. on Opt]. Instrum. Tech., Chapman and Hall, London p.305 (1961).

[5] Caroli, E. Steven, J. B., Di Cocco, G., Natalucci, L., Spizzichino, A., "Coded aperture imaging in x-ray and Gamma-ray Astronomy", Space Science Reviews, 45, 349-403 (1987).

[6] A. Haboub ; A. A. MacDowell ; S. Marchesini ; D. Y. Parkinson; Coded aperture imaging for fluorescent x-rays. Proc. SPIE 8502, Advances in X-Ray/EUV Optics and Components VII, 850209 (October 15, 2012); doi:10.1117/12.981244.

[7] Lisa P. Colletti and George J. Havrilla, "Specimen Preparation limitations in trace element analysis quantification using micro-x-ray fluorescence", Advances in X-ray Analysis, 42 (2000).

[8] Doering, D., Chuang, Y. D., Andresen, N., Chow, K., Contarato, D., Cummings, C., Domning, E., Joseph, J., Pepper, J. S., Smith, B., Zizka, G., Ford, C., Lee, W. S., Weaver, M., atthey, L., Weizeorick, J., Hussain, Z., Denes, P., "Development of a compact fast CCD camera and resonant soft x-ray scattering end station for time-resolved pump-probe experiments", Rev. Sci. Instrum. 82, 073303 - 073303-8 (2011).

DISCLAIMER

DE-AC02-05CH11231